# Photochemical Generation of a Reactive Rhenium(III) Oxo Complex and Its Curious Mode of Cleavage of Dioxygen

**Seth N. Brown[1] and James M. Mayer*[,2]**

Department of Chemistry BG-10, University of Washington, Seattle, Washington 98195

*Received March 3, 1992*

The rhenium(V) oxo oxalate complex $(HBpz_3)ReO(C_2O_4)$ ($HBpz_3$ = hydridotris(1-pyrazolyl)borato) has been synthesized in three steps from potassium perrhenate. It has been characterized spectroscopically and its molecular structure determined by X-ray crystallography. When irradiated with UV light, the oxo oxalate complex undergoes an internal redox reaction, predominantly losing carbon dioxide and generating a reactive rhenium complex. The characterization of the transient photoproduct as the rhenium(III) oxo complex $(HBpz_3)Re(O)$ is inferred from its reactions with trapping reagents: for example, photolysis in the presence of phenanthrenequinone gives a rhenium(V) oxo catecholate complex in good yield. $(HBpz_3)Re(O)$ also reacts with $O_2$, yielding the rhenium(VII) complex $(HBpz_3)ReO_3$, formally the result of four-electron oxidation. Labeling studies show that only one oxygen atom in the product comes from $O_2$, with the second deriving from an oxalate ligand. That unimolecular four-electron reduction of oxygen does not occur readily in this system, despite its great exothermicity, may be due to a general symmetry-imposed barrier to cleavage of $O_2$ at a single metal center. Crystal data for $(HBpz_3)ReO(C_2O_4)\cdot 0.5C_6H_6$: $a$ = 8.082 (2) Å, $b$ = 9.125 (3) Å, $c$ = 13.219 (3) Å, $\alpha$ = 84.03 (2)°, $\beta$ = 74.26 (2)°, $\gamma$ = 72.47 (2)°, triclinic, $P\bar{1}$, $Z$ = 2.

The terminal oxo linkage has traditionally been viewed as stabilizing high oxidation state complexes. The vast majority of stable oxo complexes are, in fact, those in which the metal is in the +4 oxidation state or higher and where the metal has two or fewer d electrons.[3] However, a growing body of recent work has demonstrated that oxo or related terminal imido ($NR^{2-}$) complexes can be stable for metals with $d^4$, $d^5$, or $d^6$ configurations and in oxidation states as low as +2.[4] These low-valent oxo or imido complexes often adopt unusual geometries to avoid antibonding interactions that would otherwise be expected between an electron-rich metal center and the strongly $\pi$-donating oxo or imido ligand.[5] In complexes where antibonding interactions are present, the metal–ligand multiple bonds are destabilized and the complexes range from mildly to exceedingly reactive.[6]

Low-valent metal–oxo complexes are of interest because they may display patterns of reactivity that differ from those of their higher-valent cousins. We set out to generate the four-coordinate rhenium(III) oxo complex, [hydridotris(1-pyrazolyl)borato]-(oxo)rhenium(III), $(HBpz_3)Re(O)$

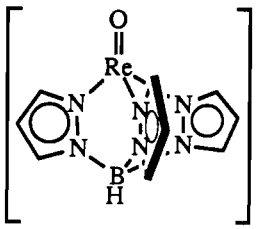

in order to explore this possibility. The pseudotetrahedral geometry that would likely be adopted by this species is known to be compatible with multiply bonded ligands in low oxidation states, as in $(RC{\equiv}CR)_2Re(O)X$,[4a,d] (ArH)Os(NR),[4e] and Cp*Ir(NR) ($Cp^* = \eta^5$-$C_5Me_5$).[4f] However, all known examples of this type are 18-electron complexes, where $(HBpz_3)Re(O)$ would have only 16 valence electrons.[7] This electronic unsaturation, coupled with the reducing rhenium(III) center, should allow the complex to undergo oxidative addition reactions, leading to stable octahedral rhenium(V) oxo complexes. Furthermore, the $d^4$ configuration of the complex might permit it to react via four-electron oxidative addition reactions:[8] for instance, oxygen could convert the rhenium(III) species to the rhenium(VII) trioxo complex $(HBpz_3)ReO_3$, a known species.[9] Such a four-electron cleavage of $O_2$ at a single metal center is currently unknown and could represent an efficient way of activating oxygen.

In this report we describe the photolysis of the rhenium(V) oxo oxalate complex $(HBpz_3)ReO(C_2O_4)$ and present evidence that the reactive transient produced on photolysis is the rhenium(III) oxo complex $[(HBpz_3)Re(O)]$. We sketch its chemistry, focusing on its deceptively simple reaction with dioxygen.

## Experimental Section

Unless otherwise noted, all procedures were performed on the benchtop without precautions to exclude air or moisture. Where necessary, standard vacuum line or inert atmosphere glovebox techniques were used. Acetonitrile and dichloromethane were dried over 4-Å molecular sieves, followed by $CaH_2$, and were vacuum transferred prior to use. Dimethyl

(1) National Science Foundation Predoctoral Fellow, 1990–1993; University of Washington Howard J. Ringold Fellow, 1989–1992.
(2) Presidential Young Investigator, 1988–1993; Sloan Foundation Fellow 1989–1991.
(3) Nugent, W. A.; Mayer, J. M. *Metal-Ligand Multiple Bonds*; Wiley-Interscience: New York, 1988.
(4) Re(III), $d^4$: (a) Mayer, J. M.; Thorn, D. L.; Tulip, T. H. *J. Am. Chem. Soc.* **1985**, *107*, 7454. (b) de Boer, E. J. M.; de With, J.; Orpen, A. G. *J. Am. Chem. Soc.* **1986**, *108*, 8271. Herrmann, W. A.; Fischer, R. A.; Amslinger, W.; Herdtweck, E. *J. Organomet. Chem.* **1989**, *362*, 333. Os(IV), $d^4$: (c) Schofield, M. H.; Kee, T. P.; Anhaus, J. T.; Schrock, R. R.; Johnson, K. H.; Davis, W. M. *Inorg. Chem.* **1991**, *30*, 3595. Re(II), $d^5$: (d) Spaltenstein, E.; Mayer, J. M. *J. Am. Chem. Soc.* **1991**, *113*, 7744. Os(II), $d^6$: (e) Michelman, R. I.; Andersen, R. A.; Bergman, R. G. *J. Am. Chem. Soc.* **1991**, *113*, 5100. Ir(III), $d^6$: (f) Glueck, D. S.; Wu, J.; Hollander, F. J.; Bergman, R. G. *J. Am. Chem. Soc.* **1991**, *113*, 2041.
(5) Mayer, J. M. *Comments Inorg. Chem.* **1988**, *8*, 125.
(6) Some leading references: (a) Che, C.-M.; Lau, K.; Lau, T.-C.; Poon, C.-K. *J. Am. Chem. Soc.* **1990**, *112*, 5176. (b) Binstead, R. A.; McGuire, M. E.; Dovletoglou, A.; Seok, W. K.; Roecker, L. E.; Meyer, T. J. *J. Am. Chem. Soc.* **1992**, *114*, 173. (c) McMurry, T. J.; Groves, J. T. In *Cytochrome P-450: Structure, Mechanism, and Biochemistry*; Ortiz de Montellano, P. R., Ed.; Plenum: New York, 1986.
(7) The analogy between $d^4$ $(HBpz_3)Re(O)$ and $d^6$ Cp*Ir(NR) is particularly close, given the electronic similarity between the cyclopentadienyl and tris(pyrazolyl)borate ligands.
(8) Bryan, J. C.; Mayer, J. M. *J. Am. Chem. Soc.* **1990**, *112*, 2298.
(9) Degnan, I. A.; Herrmann, W. A.; Herdtweck, E. *Chem. Ber.* **1990**, *112*, 1347.

0020-1669/92/1331-4091$03.00/0 

sulfoxide was dried in the same way, vacuum distilled, and stored in the glovebox. Potassium hydridotris(1-pyrazolyl)borate ($KHBpz_3$) was prepared by the procedure of Trofimenko.[10] 9,10-Dihydroxyphenanthrene was prepared from phenanthrenequinone (Aldrich) by a literature method[11] and stored in the drybox. All other reagents were commercially available and used without further purification.

$^1H$ and $^{13}C\{^1H\}$ NMR spectra were recorded on a Varian VXR-300 spectrometer at 300 and 75.4 MHz, respectively. In the descriptions of the $^1H$ NMR spectra of the compounds listed below, certain peaks are listed only as chemical shifts and multiplicity, without assignments or coupling constants. These correspond to the pyrazole protons, which appear between 5.5 and 9 ppm downfield of TMS and whose coupling constants are invariably about 2 Hz. The B–H resonance is very broad and does not vary substantially in position in diamagnetic complexes, generally appearing as a 1:1:1:1 quartet about 450 Hz wide, centered at around 4.5 ppm. This peak is not listed for the individual compounds.

IR spectra were obtained as Nujol mulls between NaCl plates on a Perkin-Elmer 1604 FT-IR spectrometer; peaks are reported in wavenumbers. The IR spectra of these compounds consist of a few bands that shift from compound to compound ($\nu_{BH}$, $\nu_{ReO}$, etc.), plus an array of pyrazolylborate bands that are quite constant, with variations of $\lesssim 5$ cm$^{-1}$. These bands are as follows (the exact values listed are those of $(HBpz_3)ReOCl_2$): 3113 (m), 1501 (m), 1406 (s), 1309 (s), 1211 (s), 1180 (m), 1119 (s), 1073 (m), 1046 (vs), 994 (w), 769 (s), 707 (m), 646 (m), 612 (m). Only the variable bands are reported for individual compounds.

Fast atom bombardment mass spectra (FABMS) were obtained using a VG 70 SEQ tandem hybrid instrument of EBqQ geometry, equipped with a standard saddle-field gun (Ion Tech Ltd., Middlesex, U. K.) producing a beam of xenon atoms at 8 keV and 1 mA. Samples were applied to the FAB target as solutions in dichloromethane or acetonitrile. Matrices used included 3-nitrobenzyl alcohol and 2-hydroxyethyl disulfide. All spectra were taken in the positive ion mode. Electron impact mass spectra were acquired on a Kratos Analytical mass spectrometer in the positive ion mode. Solid samples were loaded in direct inlet mode in melting point capillaries and were heated in vacuo to 150° to vaporize them for analysis. Gases were admitted through the reference inlet.

UV-visible spectra were obtained on a Perkin-Elmer Lambda-3B spectrophotometer. Elemental analyses were performed by Canadian Microanalytical Services, Ltd., Vancouver, BC.

**$(HBpz_3)ReOCl_2$.** This compound was prepared by a modification of the procedure of Abrams and Davison.[12] To a solution of 19.97 g $KHBpz_3$ (79.2 mmol) in 600 mL of ethanol was added 82 mL of concentrated aqueous HCl, with stirring, followed by 4.93 g $KReO_4$ (17.0 mmol). The suspension was stirred and refluxed for 2 h, during which a blue precipitate formed. The solution was cooled to room temperature and then chilled in an ice bath for 20 min. The solids were collected by suction filtration on a fritted glass funnel and washed thoroughly with 3 × 100 mL of $H_2O$ and then 2 × 50 mL of ethanol and air-dried. The yield of the sky-blue $(HBpz_3)ReOCl_2$ is 7.06 g (85%).

**$(HBpz_3)ReO(OCH_2CH_2O)$.** $(HBpz_3)ReOCl_2$ (2.50 g, 5.14 mmol), $CH_3CN$ (175 mL), and a magnetic stirbar were placed in a 250-mL round-bottom flask. After 4 equiv each of ethylene glycol (1.15 mL) and triethylamine (2.9 mL) were added the solution was refluxed, with stirring, for a day. The acetonitrile was removed from the resulting purple solution on a rotary evaporator and the residue taken up in about 50 mL of $CH_2Cl_2$. The purple solution was washed with 2 × 50 mL of $H_2O$ in a separatory funnel to remove triethylamine hydrochloride and excess ethylene glycol and then dried over $MgSO_4$. The magnesium sulfate was removed by gravity filtration and the dichloromethane distilled off on a rotary evaporator. The crude material was recrystallized from toluene/hexane, and the violet crystals were collected by suction filtration. Yield: 1.97 g (80%). $^1H$ NMR ($CD_3CN$): $\delta$ 4.76, 5.06 (m, 2 H each; $OCH_2CH_2O$); 5.98 (t, 1 H); 6.47 (t, 2 H); 7.47, 7.57 (d, 1 H each); 7.87, 8.04 (d, 2 H each). $^{13}C\{^1H\}$ NMR ($CD_3CN$): 85.3 ($OCH_2CH_2O$); 105.2, 134.8, 141.5 (pyrazole trans to oxo); 108.0, 139.0, 147.5 (pyrazoles trans to ethylene glycolate). IR: 2482 (m, $\nu_{BH}$), 958 (s, $\nu_{ReO}$); 904 (m). FABMS: $m/z$ 477 (M + H). Anal. Calcd for $C_{11}H_{14}BN_6O_3Re$: C, 27.80; H, 2.97; N, 17.68. Found: C, 27.87; H, 2.95; N, 17.67.

**$(HBpz_3)ReO(C_2O_4)$.** $(HBpz_3)ReO(OCH_2CH_2O)$ (0.527 g, 1.11 mmol) and an equimolar amount of $H_2C_2O_4 \cdot 2H_2O$ (Baker, 0.132 g) were placed in a 100-mL round-bottom flask with a magnetic stirbar. Acetonitrile (60 mL) was added and the solution stirred and heated at reflux for 2 days. The solvent was then removed on a rotary evaporator. The residue was dissolved in about 40 mL of dichloromethane and this solution carefully decanted away from a small amount of a greenish material that does not dissolve in $CH_2Cl_2$. The blue dichloromethane solution was poured into a separatory funnel and washed three times with 40 mL of $H_2O$. The organic layer was dried over $MgSO_4$, the magnesium sulfate removed by gravity filtration, and the dichloromethane removed on the rotary evaporator. The blue oil was recrystallized from ethyl acetate/hexane (one can also use toluene/hexane) to give 0.331 g (59%) of deep blue crystals. This preparation can be scaled up only with difficulty; the product obtained in larger-scale reactions is generally contaminated with a greenish material which can be removed only through repeated recrystallizations or chromatography on silica gel (eluting with EtOAc). Use of an excess of oxalic acid encourages formation of a purple, dichloromethane-insoluble byproduct and results in lower yields. $^1H$ NMR ($CD_3CN$): $\delta$ 6.04 (t, 1 H); 6.61 (t, 2 H); 7.24, 7.59 (d, 1 H each); 8.07, 8.22 (d, 2 H each). $^{13}C\{^1H\}$ NMR ($CD_2Cl_2$): $\delta$ 106.2, 136.0, 141.1 (pyrazole trans to oxo); 109.5, 140.7, 148.3 (pyrazole trans to oxalate); 161.8 ($C_2O_4$). IR: 2504 (m, $\nu_{BH}$); 1753, 1732 (s), 1676 (m) ($\nu_{CO}$); 985 (s, $\nu_{ReO}$); 812 (m). FABMS: $m/z$ 505 (M + H). UV–Vis ($CH_3CN$): $\lambda_{max}$ = 600 nm ($\epsilon$ = 80 L·mol$^{-1}$ cm$^{-1}$), 248 nm ($\epsilon = 1.1 \times 10^4$). Anal. Calcd for $C_{11}H_{10}BN_6O_5Re$: C, 26.25; H, 2.00; N. 16.70. Found: C, 26.62; H, 2.04; N, 16.75.

**$(HBpz_3)Re(O)(C_2{}^{18}O_4)$.** Anhydrous $H_2C_2O_4$ enriched in $^{18}O$ was prepared by a method used previously to prepare $^{17}O$-enriched oxalic acid.[13] The procedure used to prepare unlabeled $(HBpz_3)ReO(C_2O_4)$ was then followed, with two modifications. The reaction was conducted using the $^{18}O$-enriched anhydrous oxalic acid in place of oxalic acid dihydrate, and the reflux was carried out in dried acetonitrile under a nitrogen atmosphere. The product was worked up as described for the unlabeled material and recrystallized twice from ethyl acetate/hexane; the yield was 50%. The degree of enrichment was determined from the electron impact mass spectrum. This showed 44.6% enrichment in the $[(HBpz_3)ReO_2^+]$ fragment but no incorporation into $[(HBpz_3)ReO^+]$, indicating that the oxygen from the oxo group is the one that is retained in $[(HBpz_3)ReO^+]$ (only a very weak parent ion is observed for $(HBpz_3)ReO(C_2O_4)$). The IR spectrum shows a complex pattern in the carbonyl region (1600–1750 cm$^{-1}$), but shows no peak at 940 cm$^{-1}$ for $\nu_{Re^{18}O}$ (see below).

**$(HBpz_3)Re(^{18}O)(C_2O_4)$.** The oxo group of $(HBpz_3)ReO(C_2O_4)$ was enriched by stirring a sample with 19 equiv of $H_2{}^{18}O$ (Cambridge Isotope Labs; 98% enriched) in dry acetonitrile for 2 months at room temperature. The solvent and excess water were stripped off and the residue recrystallized as described above. Mass spectra of this material showed roughly equal enrichment in the $[(HBpz_3)ReO_2^+]$ and $[(HBpz_3)ReO^+]$ fragments, indicating that exchange occurred predominantly with the oxo group (see above) and that both fragments contain the original oxo ligand (51.2% enriched). Careful analysis showed a slightly larger $^{18}O$ incorporation in the $[(HBpz_3)ReO_2^+]$ fragment, indicating that a small amount of exchange (4.6%) occurred with the oxalate oxygens as well. IR: $\nu_{Re^{18}O}$ = 940 cm$^{-1}$ (calcd 934 cm$^{-1}$).

**$(HBpz_3)ReO(9,10\text{-phenanthrenediolate})$.** To a 50-mL round bottom flask were added $(HBpz_3)ReO(OCH_2CH_2O)$ (105 mg, 0.22 mmol) and, in the drybox, a slight excess of 9,10-phenanthrenediol (50 mg, 0.24 mmol). The flask was placed under a reflux condenser and affixed to the vacuum line. Dry acetonitrile (20 mL) was added by vacuum transfer and the solvent thawed. A light blue precipitate formed immediately, but dissolved on heating. The solution was refluxed under a nitrogen atmosphere for 5 days; even with this long reaction time, the reaction did not go to completion. The dark brown solution was opened to the air and the solvent stripped off. The residue was taken up in the minimum of $CH_2Cl_2$ and chromatographed on silica gel. The dibenzocatecholate complex elutes first as a dark brown band; removing the dichloromethane yielded 40 mg (29%) of pure $(HBpz_3)ReO(C_{14}H_8O_2)$ as a chocolate-brown powder. $^1H$ NMR ($CD_2Cl_2$): $\delta$ 5.81 (t, 1 H); 6.59 (t, 2 H); 7.19, 7.46 (d, 1 H each); 7.55, 7.66 (t, $J$ = 8 Hz, 2 H each; 2- and 3-H, phenanthrenediolate); 8.03, 8.22 (d, 2 H each); 8.39, 8.75 (d, $J$ = 8 Hz, 2 H each; 1- and 4-H, phenanthrenediolate). $^{13}C\{^1H\}$ NMR ($CD_2Cl_2$; assignments based on intensity): $\delta$ 105.9, 135.2, 139.8 (pz trans to oxo); 108.6, 139.5, 148.7 (pz trans to catecholate); 121.9, 122.8, 124.5, 126.4 (1-, 2-, 3-, and 4-C, phenanthrenediolate); 126.5, 127.9 (internal C, phenanthrenediolate), 157.1 (9-C, phenanthrenediolate). IR: 2502 (w,

(10) Trofimenko, S. *Inorg. Synth.* **1970**, *12*, 99.
(11) Oesch, F.; Sparrow, A. J.; Platt, K. L. *J. Labelled Compd. Radiopharm.* **1980**, *17*, 93.
(12) Abrams, M. J.; Davison, A.; Jones, A. G. *Inorg. Chim. Acta* **1984**, *82*, 125.
(13) Kollenz, G.; Sterk, H.; Hutter, G. *J. Org. Chem.* **1991**, *56*, 235.

$\nu_{BH}$); 1617, 1605, 1592 (w, $\nu_{CC}$ phenanthrene); 1351 (m), 1332 (m), 965 (s, $\nu_{ReO}$), 788 (m), 756 (m), 724 (m), 689 (m). FABMS: $m/z$ 624 ($M^+$). Anal. Calcd for $C_{23}H_{18}BN_6O_3Re$: C, 44.31; H, 2.91; N, 13.48. Found: C, 44.35; H, 3.00; N, 13.56.

**[{(HBpz$_3$)Re(O)}$_2$($\mu$-pz)($\mu$-O)]ReO$_4$.** To a 50-mL round-bottom flask were added 109.0 mg of (HBpz$_3$)ReOCl$_2$ (0.22 mmol), 20 mL of $CH_3CN$, 0.25 mL of $Et_3N$, 0.4 mL of $H_2O$, and a magnetic stirring bar. The solution was refluxed, with stirring, for 1.5 h, at which point all of the starting material had been consumed (by TLC). The solvent was evaporated and the oily residue dissolved in 15 mL of dichloromethane. This solution was washed with 2 × 25 mL water and dried over $MgSO_4$, and the solvent was removed on a rotary evaporator. This residue was extracted with several portions of toluene to remove the blue materials which comprise the bulk of the product of the reaction. This leaves a yellow-brown toluene-insoluble residue, which was dissolved in a small volume of acetonitrile and layered on top of several times its own volume of ethyl acetate. Glittery golden flakes deposited after the mixture was allowed to stand overnight. They were collected by suction filtration, washed with ethyl acetate and then twice with hexanes, and air-dried. Yield 5.5 mg (6%). $^1$H NMR ($CD_3CN$): $\delta$ 6.03, 6.67, 6.71 (t, 2 H each); 7.14 (t, 1 H; 4-H, $\mu$-pz); 6.61, 7.67, 8.02, 8.12, 8.26, 8.51 (d, 2 H each); 8.77 (d, 2 H; 3- and 5-H, $\mu$-pz). IR: 2531 (w, $\nu_{BH}$); 976 (s; $\nu_{ReO}$); 905 (br s, $\nu_{ReO_4}$); 733 (s). FABMS: $m/z$ 914 ($M^+$ for the cation). We have been unable to obtain analytically pure material due to the low yield of all preparations.

**General Procedure for Photolyses.** Photolyses were conducted either in sealed NMR tubes or in ordinary Pyrex glassware. The compounds to be photolyzed and any nonvolatile reagents were loaded into a flask or into an NMR tube sealed to a ground glass joint. The vessel was then attached to the vacuum line via a Teflon needle valve and evacuated, and any volatile reagents and solvents (dried and degassed) were condensed in at −77 °C. The NMR tubes were then sealed with a torch and allowed to thaw; for reactions done in flasks, the Teflon needle valve was closed. The reaction vessel was then placed in a water bath in a Pyrex beaker; reactions done in flasks were stirred magnetically. The output from a 200-W Hg(Xe) arc lamp (Oriel) was focused on the solution (with the beam passing through the beaker) for the desired length of time.

**Oxygen Labeling Experiments.** $^{18}O_2$ was obtained from Isotec (stated enrichment, 98.4%; observed enrichment by mass spectrometry, 98.1%). Photolyses were conducted under an atmosphere of oxygen as described above. After the mixtures were photolyzed for 24 h, the solvent and gases were removed on the vacuum line. Crude material for analysis by electron impact mass spectrometry was obtained by scraping the material from the flask out in the air. The solids were stored in a desiccator when not in use. If desired, they were purified by chromatography carried out on the benchtop using a Pasteur pipet filled with silica gel and eluting with $CH_2Cl_2$. This isotope patterns of the parent ion region of (HBpz$_3$)ReO$_3$ were analyzed by least-squares fitting to mixtures of the four possible isotopomers using a locally written program. Since unlabeled (HBpz$_3$)ReO$_3$ does not give the expected isotope pattern (there is a large amount of the $[M - H]^+$ fragment), the patterns of the various isotopomers were based on the empirically observed pattern of the unlabeled compound. Since it was found that samples were invariably composed of a nearly statistical distribution of the isotopomers when the amounts of the four isotopomers were allowed to refine independently, final determinations of the isotopic enrichment of the samples were based on least-square fits of the data in which the isotopomer distributions were constrained to be statistically distributed.

**Analysis of Photochemically Produced CO and CO$_2$.** Samples for which the gaseous products were to be analyzed consisted of 30–50 mg (HBpz$_3$)ReO($C_2O_4$), dissolved in dry acetonitrile containing any other desired reagents, in round-bottom flasks stoppered with Teflon needle valves. After a sample was photolyzed in the usual manner, the flask was attached to a vacuum line. The gases were collected using a Toepler pump equipped with a trap cooled in a dry ice–acetone bath to remove solvent vapors. The collected gases were then expanded into a 10-cm gas-phase IR cell with NaCl windows. The absorbance at 2360 and 2340 cm$^{-1}$ (due to $CO_2$) and at 2170 and 2120 cm$^{-1}$ (due to CO) were measured at low (4 cm$^{-1}$) resolution in a sample chamber that was purged with $N_2$ to remove atmospheric $CO_2$. Extinction coefficients were measured in independent calibrations, and Beer's law was follwed in the range 0–80 Torr for both gases: for $CO_2$, $\epsilon_{2360}$ = 1.56 (3) × 10$^{-3}$ Torr$^{-1}$ cm$^{-1}$, $\epsilon_{2340}$ = 1.33 (3) × 10$^{-3}$ Torr$^{-1}$ cm$^{-1}$; for CO, $\epsilon_{2170}$ = 1.01 (1) × 10$^{-4}$ Torr$^{-1}$ cm$^{-1}$, $\epsilon_{2120}$ = 9.43 (5) × 10$^{-5}$ Torr$^{-1}$ cm$^{-1}$.

**X-ray Structure Determination of (HBpz$_3$)ReO($C_2O_4$)·0.5$C_6H_6$.** A microcrystalline sample of (HBpz$_3$)ReO($C_2O_4$) was dissolved in dichloromethane and the solvent removed on a rotary evaporator, leaving a blue oil. This oil was dissolved in hot benzene, and, on cooling, the solution deposited well-formed blue rodlike crystals. One such crystal (0.03 × 0.12 × 0.48 mm) was glued to the tip of a glass fiber in the air. A total of 4383 reflections in four octants ($hkl$, $hk\bar{l}$, $h\bar{k}l$, $h\bar{k}\bar{l}$) with $2\theta \leq 55°$ were collected at 25 °C on an Enraf-Nonius CAD4 diffractometer using Mo K$\alpha$ radiation with a graphite monochromator ($\lambda$ = 0.710 37 Å). The crystal was triclinic and its space group was assigned as $P\bar{1}$. Crystal quality was monitored by scanning three standard reflections after approximately every 170 reflections measured. A linear correction was applied to correct for the slight (3.2%) decay that was observed. An empirical absorption correction was applied ($\mu$ = 69.21 cm$^{-1}$, transmission factors 0.997–0.754, average 0.872). After corrections for absorption and for Lorentz and polarization effects, 3797 independent reflections were obtained on averaging in $P\bar{1}$. The final data set consisted of 3027 unique observed reflections ($I > 3\sigma(I)$, $R_{av}$ = 0.025 on $F_o$).

The rhenium atom was located on a Patterson map, and remaining non-hydrogen atoms were located on subsequent difference Fourier maps. Hydrogens were fixed in calculated positions. Final full-matrix least-squares refinement converged at $R$ = 0.048 and $R_w$ = 0.056. All calculations used for the SDP/VAX package of programs supplied by the Enraf-Nonius Corp. with scattering factors and anomalous dispersion terms taken from the standard compilation.[14] Table I summarizes the crystallographic data for this compound, Table II lists selected bond distances and angles, and Table III gives fractional atomic coordinates for the refined atoms.

**Table I.** Crystallographic Data for (HBpz$_3$)ReO($C_2O_4$)·0.5$C_6H_6$

| | |
|---|---|
| $a$ = 8.082 (2) Å | formula: $C_{14}H_{13}BN_6O_5Re$ |
| $b$ = 9.125 (3) Å | fw = 542.31 |
| $c$ = 13.219 (3) Å | space group: $P\bar{1}$ |
| $\alpha$ = 84.03 (2)° | $T$ = 25 °C |
| $\beta$ = 74.26 (2)° | $\lambda$ = 0.710 73 Å |
| $\gamma$ = 72.47 (2)° | $V$ = 894.5 Å$^3$ |
| $Z$ = 2 | $\rho_{calcd}$ = 2.013 g cm$^{-3}$ |
| $\mu$ = 69.21 cm$^{-1}$ | transm coeff = 0.997–0.754 |
| $R$ = 0.048[a] | $R_w$ = 0.056[b] |
| goodness of fit = 1.239 | |

[a] $R = \Sigma||F_o| - |F_c||/\Sigma|F_o|$. [b] $R_w = [\Sigma_w(|F_o| - |F_c|)^2/\Sigma wF_o^2]^{1/2}$.

**Table II.** Selected Bond Distances (Å) and Angles (deg) in (HBpz$_3$)ReO($C_2O_4$)·0.5$C_6H_6$

| | | | |
|---|---|---|---|
| Re–O(1) | 1.654 (7) | Re–N(12) | 2.066 (7) |
| Re–O(11) | 2.007 (6) | Re–N(22) | 2.062 (7) |
| Re–O(21) | 2.000 (6) | Re–N(32) | 2.258 (7) |
| C(1)–O(11) | 1.314 (11) | C(1)–O(12) | 1.196 (12) |
| C(2)–O(21) | 1.318 (12) | C(2)–O(22) | 1.200 (11) |
| C(1)–C(2) | 1.526 (15) | | |
| O(1)–Re–O(11) | 106.1 (3) | O(11)–Re–O(21) | 80.4 (3) |
| O(1)–Re–O(21) | 104.4 (3) | O(11)–Re–N(12) | 160.6 (3) |
| O(1)–Re–N(12) | 93.1 (3) | O(11)–Re–N(22) | 90.8 (3) |
| O(1)–Re–N(22) | 94.9 (3) | O(11)–Re–N(32) | 82.7 (2) |
| O(1)–Re–N(32) | 169.4 (3) | O(21)–Re–N(12) | 92.1 (3) |
| N(12)–Re–N(22) | 90.6 (3) | O(21)–Re–N(22) | 160.3 (3) |
| N(12)–Re–N(32) | 78.5 (3) | O(21)–Re–N(32) | 82.6 (3) |
| N(22)–Re–N(32) | 78.9 (3) | | |
| Re–O(11)–C(1) | 115.4 (6) | O(11)–C(1)–O(12) | 123.1 (11) |
| Re–O(21)–C(2) | 116.0 (6) | O(21)–C(2)–O(22) | 124.1 (11) |
| O(11)–C(1)–C(2) | 114.3 (8) | O(12)–C(1)–C(2) | 122.5 (9) |
| O(21)–C(2)–C(1) | 113.2 (8) | O(22)–C(2)–C(1) | 122.8 (10) |

## Results

**Synthesis and Structure of (HBpz$_3$)ReO($C_2O_4$).** A convenient entry into tris(pyrazolyl)borate (HBpz$_3$) complexes of rhenium is offered by the known[12,15] oxo dichloride complex (HBpz$_3$)ReOCl$_2$, available in multigram quantities from potassium perrhenate and KHBpz$_3$ in a single step in high yield. When this complex is refluxed in acetonitrile containing ethylene glycol and triethylamine, ethylene glycolate replaces the two chloride ligands

(14) *International Tables for X-Ray Crystallography*; Kynoch: Birmingham, England, 1974.
(15) Degnan, I. A.; Behm, J.; Cook, M. R.; Herrmann, W. A. *Inorg. Chem.* **1991**, *30*, 2165.

**Table III.** Positional and Equivalent Isotropic Thermal Parameters for $(HBpz_3)ReO(C_2O_4)\cdot 0.5C_6H_6$

| atom | x | y | z | B,[a] Å² |
|---|---|---|---|---|
| Re | 0.22103 (5) | 0.13911 (4) | 0.35858 (3) | 3.140 (7) |
| O(1) | 0.1152 (10) | 0.1068 (8) | 0.4809 (6) | 4.9 (2) |
| O(11) | 0.2715 (8) | −0.0535 (7) | 0.2809 (6) | 4.0 (2) |
| O(12) | 0.4807 (12) | −0.2704 (9) | 0.2300 (7) | 6.2 (2) |
| O(21) | 0.4811 (9) | 0.0482 (8) | 0.3540 (6) | 4.6 (2) |
| O(22) | 0.7018 (11) | −0.1701 (10) | 0.3230 (8) | 7.0 (2) |
| N(11) | 0.1477 (10) | 0.4844 (8) | 0.3406 (7) | 3.8 (2) |
| N(12) | 0.2251 (10) | 0.3542 (8) | 0.3914 (6) | 3.7 (2) |
| N(21) | −0.0549 (9) | 0.3835 (8) | 0.2710 (6) | 3.7 (2) |
| N(22) | −0.0098 (9) | 0.2353 (8) | 0.3086 (6) | 3.4 (2) |
| N(31) | 0.2490 (10) | 0.3734 (8) | 0.1648 (6) | 3.7 (2) |
| N(32) | 0.3327 (9) | 0.2284 (8) | 0.1966 (6) | 3.3 (2) |
| C(1) | 0.4322 (14) | −0.1498 (10) | 0.2725 (9) | 4.5 (3) |
| C(2) | 0.5547 (13) | −0.0926 (12) | 0.3185 (8) | 4.5 (2) |
| C(13) | 0.2843 (14) | 0.3987 (12) | 0.4649 (9) | 4.8 (3) |
| C(14) | 0.2445 (16) | 0.5576 (13) | 0.4620 (9) | 5.6 (3) |
| C(15) | 0.1603 (15) | 0.6064 (11) | 0.3822 (10) | 5.0 (3) |
| C(23) | −0.1459 (12) | 0.1791 (11) | 0.3141 (9) | 4.1 (2) |
| C(24) | −0.2793 (12) | 0.2900 (12) | 0.2808 (9) | 4.6 (3) |
| C(25) | −0.2158 (13) | 0.4163 (12) | 0.2530 (9) | 4.4 (2) |
| C(33) | 0.4703 (13) | 0.1691 (12) | 0.1141 (9) | 4.4 (3) |
| C(34) | 0.4717 (15) | 0.2714 (14) | 0.0302 (9) | 5.4 (3) |
| C(35) | 0.3325 (15) | 0.3981 (12) | 0.0662 (9) | 5.0 (3) |
| B | 0.0865 (14) | 0.4724 (12) | 0.2418 (10) | 3.8 (3) |

[a] Anisotropically refined atoms given in the form of the isotropic equivalent thermal parameter defined as $^4/_3[a^2\beta_{11} + b^2\beta_{22} + c^2\beta_{33} + ab(\cos\gamma)\beta_{12} + ac(\cos\beta)\beta_{13} + bc(\cos\alpha)\beta_{23}]$.

**Scheme I.** Chemistry of $(HBpz_3)ReO(OCH_2CH_2O)$

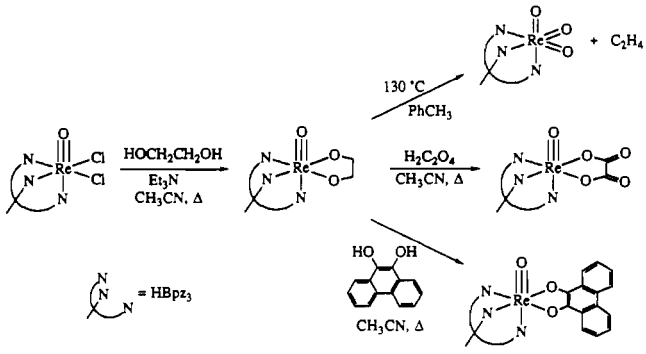


and one obtains air- and water-stable $(HBpz_3)ReO(OCH_2CH_2O)$ as a violet crystalline solid in good yield (Scheme I). The presence of two multiplets in the $^1H$ NMR and a single resonance in the $^{13}C$ NMR due to the glycolate indicates that there is a mirror plane that bisects the glycolate ligand, but that the top and bottom of the chelate ring are inequivalent. A reduction in the frequency of the rhenium–oxo stretch in the IR (958 vs 975 $cm^{-1}$ for the oxo dichloride) suggests that the lone pairs of the alkoxide oxygens compete somewhat with the terminal oxo for $\pi$ bonding to rhenium. The glycolate complex rearranges upon heating (130 °C, 4 days, toluene-$d_8$) to give ethylene and the rhenium(VII) complex $(HBpz_3)ReO_3$ (Scheme I). This reaction appears to be general for rhenium(V) oxo glycolate complexes.[16] While this work was in progress, Thomas and Davison reported an alternative synthesis of $(HBpz_3)ReO(OCH_2CH_2O)$ and noted its thermolysis to $(HBpz_3)ReO_3$.[17]

The oxo ethylene glycolate complex is a useful precursor for complexes containing chelates whose conjugate acids are more acidic than ethylene glycol (Scheme I). The oxo oxalate complex $(HBpz_3)ReO(C_2O_4)$ is formed in moderate yield by refluxing the oxo ethylene glycolate complex with 1 equiv of oxalic acid in acetonitrile for 2 days. Deep blue $(HBpz_3)ReO(C_2O_4)$ is soluble in polar organic solvents, sparingly soluble in aromatic hydrocarbons, and insoluble in hexane. The presence of oxalate is confirmed by carbonyl stretches in the IR; its bidentate binding mode is indicated by a single peak in the $^{13}C$ NMR ($\delta$ 161.8) and by a single crystal X-ray diffraction structure determination.

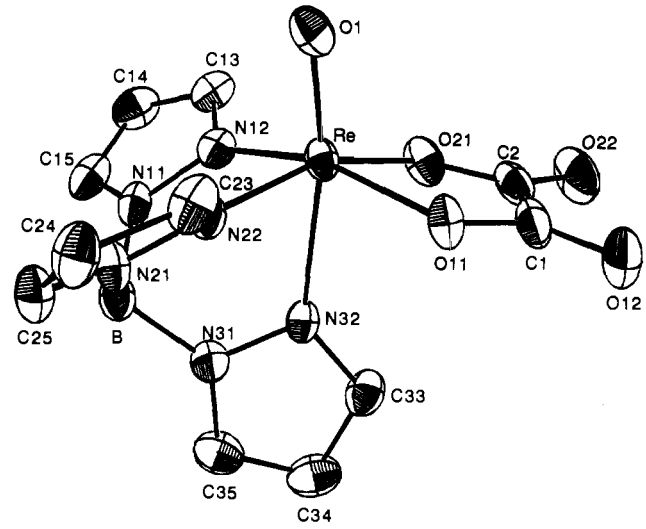


**Figure 1.** ORTEP diagram of the rhenium complex in $(HBpz_3)ReO(C_2O_4)\cdot 0.5C_6H_6$. Thermal ellipsoids are shown at the 30% level, and hydrogen atoms are omitted for clarity.

The oxalate complex is monomeric; an ORTEP diagram is shown in Figure 1. Crystallographic details are given in Table I, and selected bond distances and angles may be found in Table II. The complex crystallizes in the triclinic space group $P\bar{1}$, and a molecular of benzene sits on the inversion center. The rhenium–oxo distance, 1.654 (7) Å, is on the short end of the typical range for rhenium–oxygen triple bonds.[18] A large trans influence is observed, typical of metal–oxo complexes: the Re–N distance trans to the oxo (2.258 (7) Å) is 0.2 Å longer than those cis to the oxo (2.064 Å average). The oxalate is bound in the expected bidentate fashion, forming a five-membered ring, and the bound oxygens are bent away from the oxo more than the pyrazole nitrogens are (average 105 vs 94°). The exocyclic oxygens have much shorter C–O bonds than the endocyclic ones do (1.20 vs 1.32 Å; compare distances of 1.19 and 1.29 Å in $\alpha$-$H_2C_2O_4$[19]), suggesting that the rhenium–oxygen bonds are quite covalent. The other distances and angles in the tris(pyrazolyl)borate ligand are typical.[20]

**Photolysis of $(HBpz_3)ReO(C_2O_4)$.** In contrast to the oxo ethylene glycolate complex, the oxo oxalate complex $(HBpz_3)ReO(C_2O_4)$ is thermally robust. It can be heated to 180 °C for a month (toluene-$d_8$, sealed tube) with very little decomposition and no formation of $(HBpz_3)ReO_3$.

The oxo oxalate complex is, however, photochemically reactive. When irradiated with UV light, solutions of $(HBpz_3)ReO(C_2O_4)$ in dry acetonitrile in the absence of air gradually turn from blue to dark red-violet. The UV light may be filtered through Pyrex ($\lambda > 300$ nm), but bright visible light (through a filter that cuts off $\lambda < 455$ nm) and ambient room light (fluorescent bulbs) have no effect. Irradiation into the d–d band of the complex ($\lambda_{max}$ = 600 nm, $\epsilon$ = 80 $L\cdot mol^{-1}\ cm^{-1}$) thus does not appear to result in net photochemistry. Instead, irradiation of the UV band ($\lambda_{max}$ = 248 nm, $\epsilon = 1.1 \times 10^4$) is necessary to effect any photochemistry. This is likely a charge-transfer band involving the oxalate ligand since it is absent in the spectrum of the ethylene glycolate complex. As the photolysis of the oxalate complex proceeds, NMR signals

(16) (a) Cp*ReO($OCH_2CH_2O$): Herrmann, W. A.; Marz, D.; Herdtweck, E.; Schäfer, W.; Wagner, W.; Kneuper, H.-J. *Angew. Chem., Int. Ed. Engl.* **1987**, *26*, 462. (b) (phen)(Cl)ReO($OCH_2CH_2O$): Pearlstein, R. M.; Davison, A. *Polyhedron* **1988**, *7*, 1981.
(17) Thomas, J. A.; Davison, A. *Inorg. Chim. Acta* **1991**, *190*, 231.
(18) Mayer, J. M. *Inorg. Chem.* **1988**, *27*, 3899.
(19) Cox, E. G.; Dougill, M. W.; Jeffrey, G. A. *J. Chem. Soc.* **1952**, 4854.
(20) Thomas, R. W.; Estes, G. W.; Elder, R. C.; Deutsch, E. *J. Am. Chem. Soc.* **1979**, *101*, 4581.

**Scheme II.** Photolysis of $(HBpz_3)ReO(C_2O_4)$

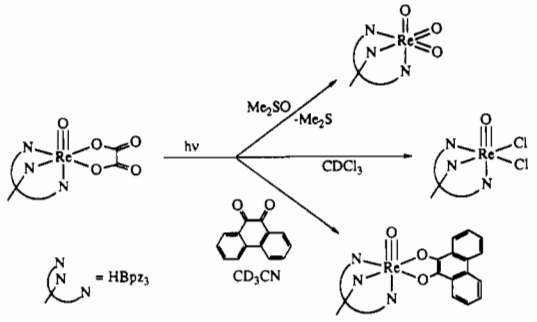


largely disappear, though small amounts of the trioxo complex $(HBpz_3)ReO_3$ are generally formed (see below). The paramagnetic product or products formed in this reaction have not been characterized. However, photolysis in the presence of certain traps does produce characterized products (Scheme II and Table IV).

Photolysis of $(HBpz_3)ReO(C_2O_4)$ in the presence of dimethyl sulfoxide yields the rhenium(VII) trioxo complex $(HBpz_3)ReO_3$ quantitatively. The observation of dimethyl sulfide, by gas-phase IR spectroscopy, indicates that oxygen atom transfer from dimethyl sulfoxide to rhenium is occurring. Varying the concentration of dimethyl sulfoxide in acetonitrile does not affect the rate of initial rate of disappearance of the oxalate complex (to 25% conversion) when solutions are photolyzed under otherwise identical conditions. Photolysis of the oxalate complex in chloroform results in the formation of $(HBpz_3)ReOCl_2$, albeit in low yields (20% by NMR).

In the presence of phenanthrenequinone, photolysis of $(HBpz_3)ReO(C_2O_4)$ in acetonitrile gives the rhenium(V) phenanthrenediolate complex $(HBpz_3)ReO(C_{14}H_8O_2)$ in good yield, 73% by NMR (Scheme II). The dibenzocatecholate complex can be prepared independently, though in modest yield, by metathesis of $(HBpz_3)ReO(OCH_2CH_2O)$ with 9,10-dihydroxyphenanthrene (Scheme I) and is isolated as an analytically pure chocolate brown powder after chromatography on silica gel. The complex is monomeric by mass spectrometry, and $^1H$ and $^{13}C$ NMR spectra establish the presence of a plane of symmetry in the molecule, consistent with a structure similar to the oxalate complex.

The primary photoprocess thus appears to be loss of the oxalate as two molecules of $CO_2$ and the formation of $(HBpz_3)Re(O)$, which is trapped by oxygen atom transfer (to give $[HBpz_3]ReO_3$), by chlorine atom transfer (to give $[HBpz_3]ReOCl_2$), or by phenanthrenequinone to give the dibenzocatecholate complex. Photolyses also invariably produce small amounts (5–15%) of the trioxo complex $(HBpz_3)ReO_3$, suggesting that there is a secondary pathway for photochemical fragmentation, to directly form the trioxo complex and two molecules of CO (Scheme III). Carbon monoxide and carbon dioxide are both observed by gas-phase IR analysis of the headspace of the photochemical reactions (see below).

All of the effective traps described above act as oxidizing agents, forming rhenium(V) or rhenium(VII) products. Reactions with traps that are not oxidizing agents have so far failed to yield diamagnetic products. Examples of such ineffective traps include CO and $^t$BuNC, which could potentially deoxygenate a rhenium(III) oxo complex and stabilize the rhenium(I) center that would result, and 2,2′-bipyridine, MeC≡CMe, and PhC≡CPh, ligands that might bind well to a low-valent complex (note that Cp*Re(O)(RC≡CR) is a stable species[4b]). $CH_3SSCH_3$, $CH_3I$, biacetyl, diethyl azodicarboxylate, and ethylene oxide also fail to produce significant amounts of diamagnetic products even though they are oxidizing agents, so the distinction between successful and unsuccessful traps is not clear-cut.

**Photolysis of $(HBpz_3)ReO(C_2O_4)$ in the Presence of Dioxygen.** Photolysis of the oxo oxalate complex in the presence of $O_2$ results

**Scheme III**

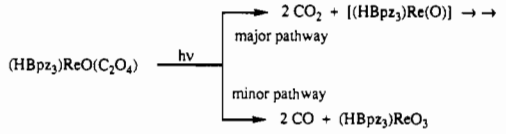


in the formation of the rhenium(VII) trioxo complex $(HBpz_3)ReO_3$. The reaction is essentially quantitative at high oxygen pressures or low concentrations of $(HBpz_3)ReO(C_2O_4)$, as summarized in Table IV.

In photolyses carried out in more concentrated solutions and at lower oxygen pressures, a diamagnetic side product appears at the expense of formation of $(HBpz_3)ReO_3$. This yellow-brown product can be isolated in low yield by chromatography of the reaction mixtures or can be isolated as a low-yield byproduct in the base hydrolysis of $(HBpz_3)ReOCl_2$. We tentatively identify this product as the rhenium(V) dimer $[(HBpz_3)_2Re_2(O)_2(\mu\text{-}O)(\mu\text{-}pz)]ReO_4$ on the basis of spectroscopic evidence. The FAB mass spectrum exhibits a very strong peak at $m/z$ = 914, corresponding to the mass of the cation, with the isotope pattern expected for a species with two rhenium and two boron atoms. The $^1H$ NMR spectrum of this diamagnetic compound consists of three triplets and six doublets, all of equal intensity, which is the usual pattern exhibited by a tris(pyrazolyl)borate ligand bound to a rhenium whose three other ligands are all distinct. In addition, there is a low-field doublet, of the same intensity as each of the tris(pyrazolyl)borate resonances, which is coupled to a triplet with half its intensity. This indicates that there is one additional pyrazolyl group per two tris(pyrazolyl)borate ligands, and that it is bound symmetrically. The IR spectrum shows a strong sharp band characteristic of a rhenium(V) terminal oxo moiety ($\nu$ = 976 $cm^{-1}$); a strong broad band at 905 $cm^{-1}$ suggests the presence of perrhenate anion (c.f. $\nu_{ReO_4^-}$ = 897 $cm^{-1}$ in $KReO_4$).

The yield of the dimeric side product varies in a systematic way with the reaction conditions. Both the oxygen pressure and the concentration of $(HBpz_3)ReO(C_2O_4)$, taken together, seem to be important: the ratio of $[(HBpz_3)_2Re_2(O)_2(\mu\text{-}O)(\mu\text{-}pz)]ReO_4$ to $(HBpz_3)ReO_3$ increases as the ratio of rhenium concentration to oxygen pressure increases (Figure 2). This crude but unmistakable correlation indicates that there is a branch point in the reaction where some intermediate can react either with a molecule of oxygen, leading ultimately to the formation of $(HBpz_3)ReO_3$, or with a molecule of $(HBpz_3)ReO(C_2O_4)$, leading ultimately to the formation of the rhenium(V) dimer $[(HBpz_3)_2Re_2(O)_2(\mu\text{-}O)(\mu\text{-}pz)]ReO_4$.

The details of the reaction with $O_2$ to give $(HBpz_3)ReO_3$ have been examined by a variety of labeling experiments. Photolysis of acetonitrile solutions of $(HBpz_3)ReO(C_2O_4)$ under an atmosphere of $^{18}O_2$ produces $(HBpz_3)ReO_3$ whose isotopic composition is doubly remarkable. First, mass spectra of isotopically enriched $(HBpz_3)ReO_3$ invariably show an isotope pattern consistent with a statistical distribution of all possible isotopomers from unlabeled to trilabeled (e.g., Figure 3). Scrambling of oxygens between molecules of $(HBpz_3)ReO_3$ occurs even when a solid sample enriched in $^{18}O$ is physically mixed with a solid sample of unlabeled material and the powder is heated to 150 °C to vaporize it for mass spectral analysis. The facility of this exchange process is noteworthy in itself, but in this context it has the unfortunate consequence of washing out the intimate details of the fate of the oxygen atoms. The only mechanistic information that can be obtained under these conditions is the overall degree of enrichment, which is the second surprising feature.

We anticipated that the photolysis would proceed predominantly as outlined in eq 1, with the photogenerated rhenium(III) intermediate acquiring both oxygen atoms from $O_2$. If this were the case, the degree of enrichment of the $(HBpz_3)ReO_3$ formed in the presence of $^{18}O_2$ would be about 67%. In fact, the observed degree of enrichment is only 29% (Table V). This finding is

**Table IV.** Photochemical Reactions of $LReO(C_2O_4)$ ($L = (HBpz_3)^-$)

| conditions | photolysis time, h | % conversion[a] | products (% yield, based on converted material)[a] |
|---|---|---|---|
| DMSO-$d_6$ | 26 | 100 | $LReO_3$ (100) |
| $CDCl_3$ | 22 | 94 | $LReOCl_2$ (20)<br>$LReO_3$ (4) |
| phenanthrenequinone (2.2 equiv)<br>$CD_3CN$ | 88 | 55 | LReO(phenanthrenediolate) (73)<br>$LReO_3$ (14) |
| $O_2$ (~500 Torr)[b]<br>$CD_3CN$<br>$[LReO(C_2O_4)]_0 = 29$ mM | 24 | 88 | $LReO_3$ (33)<br>$[(LReO)_2(\mu\text{-pz})(\mu\text{-O})]ReO_4$ (40) |
| $O_2$ (~500 Torr)[b]<br>$CD_2Cl_2$<br>$[LReO(C_2O_4)]_0 = 24$ mM | 11 | 90 | $LReO_3$ (41)<br>$LReOCl_2$ (3)<br>$[(LReO)_2(\mu\text{-pz})(\mu\text{-O})]ReO_4$ (4) |
| $O_2$ (~3 atm)[b]<br>$CD_3CN$<br>$[LReO(C_2O_4)]_0 = 31$ mM | 24 | 83 | $LReO_3$ (81)<br>$[(LReO)_2(\mu\text{-pz})(\mu\text{-O})]ReO_4$ (6) |
| $O_2$ (710 Torr)<br>$CH_3CN$<br>$[LReO(C_2O_4)]_0 = 5.9$ mM | 25 | 73 | $LReO_3$ (47)<br>$[(LReO)_2(\mu\text{-pz})(\mu\text{-O})]ReO_4$ (21) |
| $O_2$ (714 Torr)<br>$CH_3CN$<br>$[LReO(C_2O_4)]_0 = 1.1$ mM | 22 | 100 | $LReO_3$ (~100)<br>$[(LReO)_2(\mu\text{-pz})(\mu\text{-O})]ReO_4$ (6) |

[a] Yields and coversions of reactions in deuterated solvents were calculated by integration of $^1H$ NMR signals relative to internal standards, typically added $C_6H_6$ or TMS or residual protons of the solvent. Yields and conversions of reactions in protio solvents were obtained by adding a weighed amount of ferrocene to the crude reaction mixture, removing the solvent from an aliquot, and comparing the integrated NMR signals of the product to that of the ferrocene. [b] Gas pressures in sealed NMR tubes were not measured directly; the values are estimated on the basis of the manner of preparation of the samples.

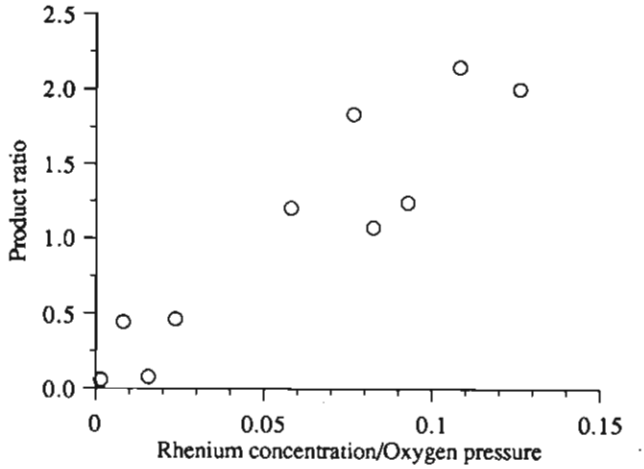


**Figure 2.** Ratio of the yields of $[(HBpz_3)_2Re_2(O)_2(\mu\text{-O})(\mu\text{-pz})](ReO_4)$ to $(HBpz_3)ReO_3$ as a function of the ratio of the initial concentration of $(HBpz_3)ReO(C_2O_4)$ (mM) to oxygen pressure (Torr) in the photochemical oxygenation of the oxo oxalate complex $(HBpz_3)ReO(C_2O_4)$ in acetonitrile.

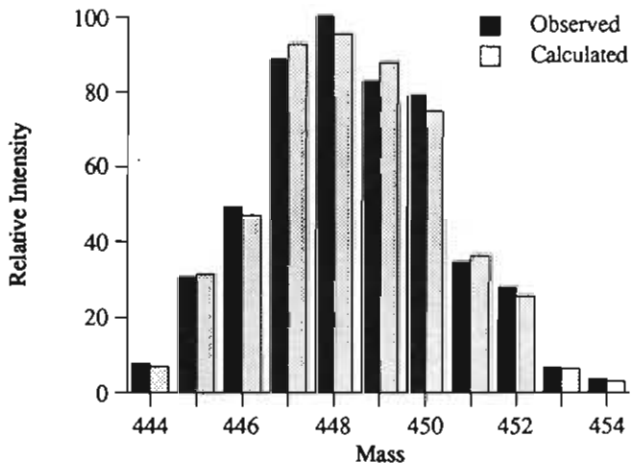


**Figure 3.** Observed and calculated isotope pattern for the mass spectrum of an isotopically enriched sample of $(HBpz_3)ReO_3$. The calculated pattern is based on 28.9% overall $^{18}O$ enrichment, with the following statistical distribution of the four isotopomers: 35.9% $(HBpz_3)Re(^{16}O)_3$, 43.8% $(HBpz_3)Re(^{16}O)_2(^{18}O)$, 17.8% $(HBpz_3)Re(^{16}O)(^{18}O)_2$, and 2.4% $(HBpz_3)Re(^{18}O)_3$.

$$(HBpz_3)ReO(C_2O_4) \xrightarrow[-2CO_2]{h\nu} [(HBpz_3)Re(O)] + O_2 \rightarrow (HBpz_3)ReO_3 \quad (1)$$

quite robust. The enrichment is essentially unchanged when the concentration of $(HBpz_3)ReO(C_2O_4)$ is increased by a factor of 6, though this changes the yield of $(HBpz_3)ReO_3$ from ca. 100% to 47%. The degree of incorporation of $^{18}O$ scales with the degree of enrichment of the oxygen gas used: when the reaction is conducted under an atmosphere of 43% $^{18}O_2$/57% $^{16}O_2$, the enrichment of the $(HBpz_3)ReO_3$ falls to 12%, which is 42% of the enrichment observed under pure $^{18}O_2$. It is unlikely that the low enrichments are the result of loss of $^{18}O$ label by exchange with atmospheric air or with water, in light of the reproducibility of the enrichments. Purification of the material on silica gel, a procedure likely to accelerate any exchange with water, has no effect on the observed incorporation of $^{18}O$.

The observed 29% enrichment is close to one-third, the value one would expect if only one of the three oxo groups in $(HBpz_3)ReO_3$ came from $O_2$. The difference reflects the small amount of direct formation of $(HBpz_3)ReO_3$ on photolysis of the oxalate complex even in the absence of oxygen (Scheme III) which does not lead to any $^{18}O$ incorporation. The data imply that 13% of the $(HBpz_3)ReO_3$ is formed by the $O_2$-independent pathway, consistent with the 5–15% $(HBpz_3)ReO_3$ typically observed on photolysis of the oxalate in the absence of oxygen (see above).

To trace the source of the remainder of the oxo groups, we prepared samples of $(HBpz_3)ReO(C_2O_4)$ with $^{18}O$ enriched in either the oxo group or the oxalate ligand: the former generated by exchange with labeled water, the latter prepared using $^{18}O$-oxalic acid.[13] The amount of enrichment has been determined from mass spectra using the isotope patterns for the fragments at $m/z = 416$ $[(HBpz_3)ReO^+]$ and 432 $[(HBpz_3)ReO_2^+]$ (see Experimental Section). These two independently enriched

**Table V.** Oxygen-18 Labeling Results for

$$(HBpz_3)ReO(C_2O_4) + O_2 \xrightarrow[CH_3CN]{h\nu} (HBpz_3)ReO_3$$

| concn of $(HBpz_3)ReO(C_2O_4)$, mM | enriched component (% $^{18}O$) | % $^{18}O$ in $(HBpz_3)ReO_3$ | % oxygen contribn to $(HBpz_3)ReO_3$ |
|---|---|---|---|
| 6.20 | $O_2$ (98.1 (3)) | 28.5 (10) | 29.1 (10) |
| 0.97 | $O_2$ (98.1 (3)) | 30.1 (6) | 30.7 (6) |
| 6.32 | $O_2$ (43.0 (1)[a]) | 12.2 (7) | 28 (2) |
| 0.93 | $(HBpz_3)Re\mathit{O}(C_2O_4)$ (55.8 (12)[b]) | 19.0 (6) | 34 (1) |
| 1.0 | $(HBpz_3)ReO(C_2\mathit{O}_4)$ (44.5 (13)) | 14.6 (8) | 33 (2) |

[a] Prepared by mixing 98% enriched $^{18}O_2$ and unlabeled $^{16}O_2$; the total isotopic enrichment was determined by mass spectrometry. [b] This material was 51.2% enriched in the oxo group and 4.6% enriched in the oxalate.

samples of $(HBpz_3)ReO(C_2O_4)$ were photolyzed in acetonitrile in the presence of $^{16}O_2$ gas, and the $(HBpz_3)ReO_3$ product was analyzed by mass spectrometry. In each case, one-third of the oxygen in the product came from the labeled site (Table V).

The labeling study forces one to draw the rather odd conclusion that each of the three oxygens in the $(HBpz_3)ReO_3$ formed by aerobic photolysis of $(HBpz_3)ReO(C_2O_4)$ comes from a different source: one from the original oxo, one from the oxalate ligand, and one from the added oxygen gas. Thus, the stoichiometry of the reaction conforms to eq 2, rather than to the anticipated

$$(HBpz_3)ReO(C_2O_4) + {}^1/_2O_2 \xrightarrow{h\nu} (HBpz_3)ReO_3 + CO + CO_2 \quad (2)$$

stoichiometry of eq 1. Confirmation of the stoichiometry comes from an analysis of the volatiles from the reaction by gas-phase IR, showing a ratio of $CO_2$ to CO of 0.69 (3), corresponding to a 41:59 mixture of $CO_2$:CO. This is in excellent agreement with the 1:1 ratio of eq 2, augmented by a slight surplus of CO produced by the oxygen-independent photochemical path to $(HBpz_3)ReO_3$ from $(HBpz_3)ReO(C_2O_4)$ (Scheme III). Indeed, the 13% of direct reaction calculated from the $^{18}O_2$ labeling results imply a $CO_2$/CO ratio of 0.77(5) (44:56), in remarkably good agreement with the IR data. This quantitative agreement should, however, be treated with caution because photolysis under other conditions leads to unexpectedly high amounts of CO. Photolysis of $(HBpz_3)ReO(C_2O_4)$ in acetonitrile in the absence of any other reagents produces a 50:50 mixture of $CO_2$ and CO, a result that is difficult to interpret since the products of this reaction are unknown. In the presence of dimethyl sulfoxide, which appears to be an excellent trap for the photogenerated species, photolysis gives 1.78 (4):1 or 64:36 mixture of $CO_2$ and CO, much more CO than would be expected from the NMR and labeling experiments (roughly 87:13). Nevertheless, the counterintuitive result is qualitatively clear: in the presence of oxygen, certainly an oxidizing agent, more of the more reduced gas, carbon monoxide, is released.

## Discussion

**Photochemistry of $(HBpz_3)ReO(C_2O_4)$.** The major pathway of photolysis of the oxo oxalate complex $(HBpz_3)ReO(C_2O_4)$ appears to involve generation of 2 equiv of $CO_2$ and the rhenium(III) monooxo complex $(HBpz_3)Re(O)$, as depicted in Scheme III. This is inferred from the products observed when the photolysis is carried out in the presence of trapping agents, in particular the high-yield production of the oxo catecholate complex $(HBpz_3)ReO(C_{14}H_8O_2)$ in the presence of phenanthrenequinone. There also appears to be a minor pathway involving loss of 2 equiv of carbon monoxide from $(HBpz_3)ReO(C_2O_4)$ and formation of $(HBpz_3)ReO_3$ (Scheme III), as some of the trioxo product is invariably formed on photolysis, regardless of the trapping agent. This in part explains why both CO and $CO_2$ are produced in the reactions. The results are also consistent with direct photochemical production of both CO and $CO_2$ together with $[(HBpz_3)ReO_2]$, followed by an unusual disproportionation to $(HBpz_3)ReO_3$ and $[(HBpz_3)Re(O)]$. We think this pathway unlikely on the basis of the related chemistry of reduction of $(HBpz_3)ReO_3$ by $PPh_3$,[15] which apparently generates $(HBpz_3)ReO_2$, but the subsequent chemistry is not similar to that observed here.[21]

Photochemical oxidation of oxalate to carbon dioxide is a common feature of the photochemistry of transition metal oxalate complexes. Two-electron reduction of a single metal center with loss of two $CO_2$ molecules and formation of an unsaturated complex, as in the major path of Scheme III, have been observed in the generation of $[(R_3P)_2Pt^0]$ from $(R_3P)_2Pt(C_2O_4)$[22] and the generation of $[Cp^*Ir(PR_3)]$ from $Cp^*Ir(PR_3)(C_2O_4)$.[23] The (one-electron) photoreduction of first-row transition complexes such as $Fe(C_2O_4)_3^{3-}$ and $Co(C_2O_4)_3^{3-}$ has been known for many years.[24] On the other hand, the minor process observed here, photochemical *reduction* of oxalate to carbon monoxide, is to our knowledge unprecedented. Oxalate is a poor oxidant, so the fact that this pathway does occur here, even in minor amounts, attests to the ease of oxidation of the rhenium center to $(HBpz_3)ReO_3$.

**Reactivity of Photogenerated $[(HBpz_3)Re(O)]$.** We describe the reactive transient generated on photolysis of $(HBpz_3)ReO(C_2O_4)$ as $[(HBpz_3)Re(O)]$, although there is no direct evidence for this species. We favor a pseudotetrahedral geometry by analogy with the four-coordinate bis(acetylene)rhenium(III) oxo complexes $(RC{\equiv}CR)_2Re(O)X$ (X = halide, alkyl, etc.), where the stability of the oxo moiety has been attributed to their unusual pseudo-3-fold symmetry.[4a]

$[(HBpz_3)Re(O)]$ acts as a reducing agent, reasonable reactivity for an unsaturated or labile rhenium(III) oxo complex without $\pi$-acid ligands. The oxo group of the intermediate does not appear to be particularly activated, as it is retained in all of the products we have identified so far. The observation that a variety of inner-sphere oxidants, including $CH_3SSCH_3$, $CH_3I$, biacetyl, and diethyl azodicarboxylate, are not effective traps suggests that $[(HBpz_3)Re(O)]$ has an unexpectedly subdued degree of reactivity. We suggest that this is due not to an intrinsic lack of reactivity but to its unexpectedly high reactivity toward its precursor, $(HBpz_3)ReO(C_2O_4)$. The amount of CO produced on photolysis of the oxo oxalate complex is larger in the absence of an added trap (CO:$CO_2$ = 50:50 on photolysis in $CH_3CN$), indicating that more oxalate is being reduced, presumably by $[(HBpz_3)Re(O)]$. The pattern of product distribution in the photolysis of $(HBpz_3)ReO(C_2O_4)$ in the presence of oxygen also points to the possibility of $(HBpz_3)Re(O)$ reacting with the oxo oxalate complex. Thus it seems likely that, in the absence of an effective trap, photogenerated $(HBpz_3)Re(O)$ reacts in some manner with $(HBpz_3)ReO(C_2O_4)$ to form the uncharacterized dark red-violet paramagnetic product(s). The oxalate ligand was intended as an innocent source of reducing power, but in fact it participates actively in the observed chemistry, masking the reactivity of the reduced complex toward substrates less reactive than the oxo oxalate precursor.

(21) The evidence for initial formation of $(HBpz_3)ReO_2$ is the observation of $Ph_3PO$ and, in the presence of trimethylsilyl halides, formation of $(HBpz_3)ReOX_2$[15] and $(Me_3Si)_2O$. In the absence of silyl halides, the fate of $(HBpz_3)ReO_2$ is not similar to the decomposition observed here. In particular, the trioxo complex is fully consumed upon reaction with 1 equiv of phosphine; if disproportionation of the dioxo complex were facile, one would expect half of the $(HBpz_3)ReO_3$ to remain under these conditions.

(22) Blake, D. M.; Nyman, C. J. *J. Am. Chem. Soc.* **1970**, *92*, 5329. Paonessa, R. S.; Prignano, A. L.; Trogler, W. C. *Organometallics* **1985**, *4*, 647.
(23) Freedman, D. A.; Mann, K. R. *Inorg. Chem.* **1991**, *30*, 836.
(24) Adamson, A. W.; Waltz, W. L.; Zinato, E.; Watts, D. W.; Fleischauer, P. D.; Lindholm, R. D. *Chem. Rev.* **1968**, *68*, 541.

**Scheme IV**

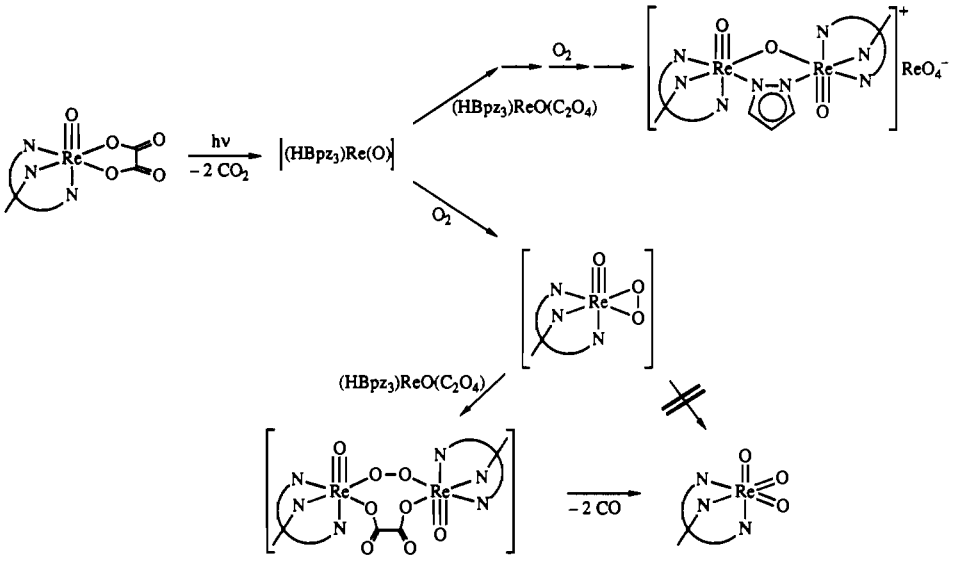

**Mechanism of the Reaction with Dioxygen.** $(HBpz_3)ReO(C_2O_4)$ is inert to oxygen in the dark, so a photochemical event must precede any subsequent reactions. The photolytically generated species is most likely $(HBpz_3)Re(O)$, as discussed above. This species is an excellent candidate to undergo the branching demanded by the product distribution data (see Results and Figure 2). At high concentrations of $(HBpz_3)ReO(C_2O_4)$ or at low oxygen pressure, $(HBpz_3)Re(O)$ is trapped by the oxo-oxalate starting material, as described immediately above. In the absence of oxygen or other traps, this likely leads to the red-violet paramagnetic material. In the presence of oxygen, this path appears to lead to $[(HBpz_3)_2Re_2(\mu\text{-}O)(\mu\text{-}pz)](ReO_4)$ (Scheme IV). At high oxygen pressures or low initial concentrations, $(HBpz_3)Re(O)$ is trapped by oxygen, initiating the pathway to $(HBpz_3)ReO_3$. This reaction forms a species with the stoichiometry $(HBpz_3)ReO(O_2)$, presumably an $\eta^2$-peroxo complex of rhenium(V) (Scheme IV). This two-electron oxidative addition of $O_2$ is reminiscent of the addition of quinone to $(HBpz_3)Re(O)$, and the $\eta^2$-peroxo ligand is related to the $\eta^2$-oxalate, -glycolate, and -catecholate species. Addition of $O_2$ to second- and third-row transition metals often results in peroxo complexes,[25] and a stable rhenium peroxo compound has been prepared by this route.[26]

It should be noted that our evidence for the intermediacy of $[(HBpz_3)ReO(O_2)]$ is strong but not conclusive. Neither this species nor its precursor, $[(HBpz_3)Re(O)]$, has been directly observed. The fate of the likely peroxo intermediate is, however, of considerable interest because it does not simply rearrange to isomeric $(HBpz_3)ReO_3$. Instead, the observed incorporation of an oxygen from an oxalate ligand implies that the oxo peroxo complex interacts with a molecule of $(HBpz_3)ReO(C_2O_4)$ before forming the trioxo complex. Scheme IV summarizes the mechanistic arguments and presents a possible structure for a dimeric intermediate (although speculative, a similar structure has been proposed in a cobalt system[27]). Cleavage of both the peroxide and the oxalate ligand in the dinuclear species would generate $(HBpz_3)ReO_3$ and CO with the proper stoichiometry and labeling.

Thermodynamic considerations cannot explain the failure of the peroxo ligand to cleave its O–O bond (eq 3a), for it is certainly enormously favorable energetically, as can be seen by a comparison of eqs 3 and 4. The oxo ethylene glycolate complex $(HBpz_3)ReO(OCH_2CH_2O)$ is observed to be converted upon heating

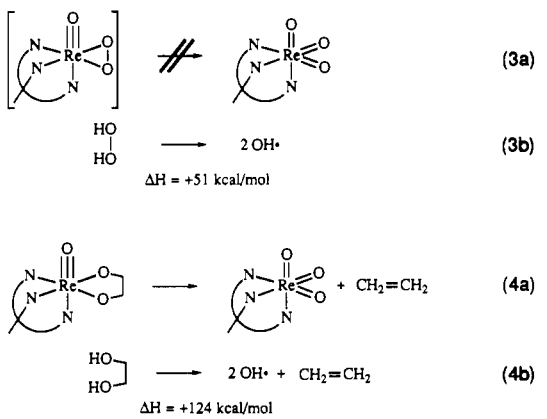

(3a)

(3b)

$\Delta H$ = +51 kcal/mol



(4a)

(4b)

$\Delta H$ = +124 kcal/mol

to the trioxo complex $(HBpz_3)ReO_3$ and ethylene (eq 4a) in spite of ethylene glycol being a very poor oxidant, as revealed by its highly endothermic conversion to ethylene and two OH• moieties (eq 4b).[28] Hydrogen peroxide, on the other hand, is an excellent oxidant: in the gas phase it is *70 kcal/mol* better able to generate two hydroxyl radicals than is ethylene glycol (eq 3b).[28] This enormous difference in oxidizing power must carry over into the rhenium system,[29] indicating that rearrangement of $(HBpz_3)ReO(O_2)$ to $(HBpz_3)ReO_3$ (eq 3a)—simply breaking the O–O bond—must be tremendously exothermic.

There is apparently a substantial kinetic barrier to the four-electron cleavage of dioxygen at a single rhenium center. A possible origin for this barrier is suggested by the results of a study of the photochemical production of $O_2$ from permanganate ion,[30] in which a long-lived intermediate was tentatively assigned as a manganese(V) peroxo complex. The relatively long lifetime of this species was attributed to a symmetry-forbidden orbital crossing in the conversion of the manganese(V) peroxo species back to permanganate. Although the argument was enunciated specifically for the case of permanganate, we expect that it should apply generally to the interconversion of $d^2$ metal peroxides and

(25) Vaska, L. *Acc. Chem. Res.* **1976**, *9*, 175.
(26) Nicholson, T.; Zubieta, J. *Inorg. Chim. Acta* **1987**, *134*, 191–3.
(27) $[(BISDIEN)_2Co_2(\mu\text{-}OH)(\mu\text{-}O_2)(\mu\text{-}C_2O_4)]^+$ (BISDIEN = $[(CH_2CH_2NH)_3(CH_2CH_2O)]_2$): Martell, A. E.; Motekaitis, R. J. *J. Am. Chem. Soc.* **1988**, *110*, 8059.
(28) Thermodynamic data taken from: Chase, M. W., Jr.; Davies, C. A.; Downey, J. R., Jr.; Frurip, D. J.; McDonald, R. A.; Syverud, A. N. *JANAF Thermochemical Tables*, 3rd ed.; American Institute of Physics: New York, 1986. Excepted are data for ethylene glycol, which are from: Pedley, J. B.; Naylor, R. D.; Kirby, S. P. *Thermochemical Data of Organic Compounds*, 2nd ed.; Chapman and Hall: New York, 1986. $\Delta H$ values are for gas phase reactions at 298 K.
(29) The presumably favorable entropy for the decomposition of the ethylene glycolate complex might offset some slight endothermicity, but not on the scale of dozens of kilocalories per mole.
(30) Lee, D. G.; Moylan, C. R.; Hayashi, T.; Brauman, J. I. *J. Am. Chem. Soc.* **1987**, *109*, 3003.

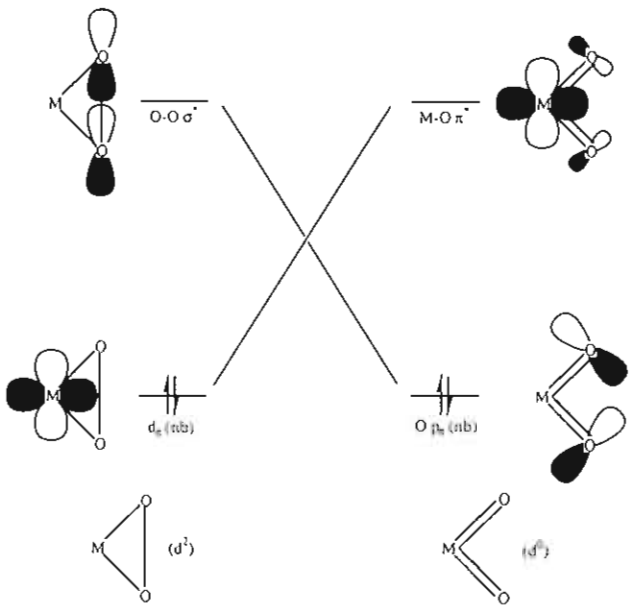


**Figure 4.** Qualitative correlation diagram for the conversion of a $d^2$ metal peroxo complex to a $d^0$ dioxo complex.

$d^0$ *cis*-dioxo species[31] (see Figure 4). The pair of metal d electrons in the $d^2$ peroxide must be transferred to the O–O $\sigma^*$ orbital in order to break the O–O bond; these electrons become an oxygen lone pair combination in the $d^0$ product. In octahedral geometries where the peroxo group occupies two coordination sites, the only d orbital that is of the same symmetry as the O–O $\sigma^*$ orbital is metal–ligand $\sigma$-antibonding, and thus empty in a $d^2$ complex. Because the filled d orbital in the peroxo complex and the O–O $\sigma^*$ orbital are of different symmetries, transfer of the electrons from the metal to the peroxide is symmetry-forbidden. In the specific case of a cis $d^2$ oxo–peroxo complex, such as $(HBpz_3)ReO(O_2)$ (as illustrated in Figure 4), the two d electrons would occupy the $d_\pi$ orbital in the plane of the peroxo ligand, since this is invariably the occupied orbital in $d^2$ metal oxo complexes.[3]

The generality of this argument is supported by several instances in the literature, where molecules could undergo analogous reactions but fail to do so for reasons that are not immediately apparent. The most striking example is the molybdenum–nitrosobenzene adduct $(Et_2NCS_2)_2Mo(\eta^2\text{-PhNO})$, which does not rearrange, either thermally or photochemically, to give the known oxo imido complex $(Et_2NCS_2)_2Mo(NPh)(O)$ (eq 5).[32]

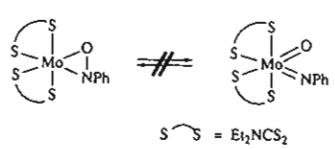


$$\not\rightleftharpoons \qquad (5)$$

S⌒S = $Et_2NCS_2$

Similarly, decomposition of the aqueous species $Cr(O_2)^{2+}$ to "$Cr(O)_2^{2+}$" (that is, chromate), occurs only via a bimolecular path.[33] The stability of the rhenium peroxo complex $Re(O_2)(NNCO_2Me)Cl_2(PPh_3)_2$ is also noteworthy in this context.[26] It is interesting to contrast the rarity of unimetallic cleavage of peroxide to two oxo groups with the well-documented bimetallic analog, M—O—O—M → M=O + O=M.[34]

Curiously, the two examples of peroxide cleavage at a single metal center that we are aware of both involve reactions of $d^0$ peroxide complexes. A bis(peroxo) porphyrin complex of molybdenum(VI) is photochemically converted to the *cis*-dioxo complex and free $O_2$,[35] although the mechanism has not been established[36] (eq 6; TTP = *meso*-tetra-*p*-tolylporphyrin). Most

$$(TTP)Mo(O_2)_2 \xrightarrow{h\nu} \textit{cis}\text{-}(TTP)Mo(O)_2 + O_2 \qquad (6)$$

relevant is the observation that dilute solutions of $Mo(O^tBu)_4$ react with oxygen to give $MoO_2(O^tBu)_2$ and *tert*-butoxy radicals (eq 7).[37] The reaction appears to be unimolecular, since in more

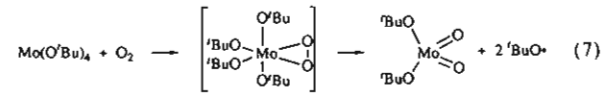


(7)

concentrated solution the product is $MoO(O^tBu)_4$, as expected for bimolecular oxygen activation. The remarkable transformation in eq 7 clearly demonstrates the extreme thermodynamic drive toward oxygen–oxygen bond cleavage in appropriate systems: scission to the dioxo moiety takes place spontaneously even at the expense of homolysis of two Mo–O single bonds to alkoxy radicals. The kinetic requirements of the bond cleavage reaction also become apparent when the facile reaction in eq 7 is contrasted to the apparently similar, but unobserved, rearrangements of $(Et_2NCS_2)_2Mo(ONPh)$ (eq 5) or $(HBpz_3)ReO(O_2)$ (Scheme IV). That a $d^0$ metal center is able to act as a reducing agent where a $d^2$ metal cannot is a baffling observation, except in the light of the symmetry restriction addressed above. The alkoxide complex can draw on a metal–ligand $\sigma$-bonding orbital of the same symmetry as the peroxide $\sigma^*$ orbital to allow a concerted transfer of electrons, while the occupied d orbital of $(Et_2NCS_2)_2Mo(ONPh)$ or $(HBpz_3)ReO(O_2)$ is prevented from participating in such a reaction by virtue of its symmetry.[38]

## Conclusions

Photolysis of the stable rhenium(V) oxo oxalate complex, $(HBpz_3)ReO(C_2O_4)$, generates a reactive transient, the rhenium(III) terminal oxo complex $(HBpz_3)Re(O)$. This intermediate is trapped by certain inner-sphere oxidants—e.g., dimethyl sulfoxide, chloroform, and phenanthrenequinone—to give stable rhenium(V) or rhenium(VII) products. Reactivity at the oxo ligand has not been observed. The oxo oxalate precursor also reacts with the photochemically generated complex, which limits

(31) In general, *cis*-dioxo complexes are only stable for $d^0$ electron configurations,[3] so this is the critical case to consider. For some exceptions, see: Ram, M. S.; Hupp, J. T. *Inorg. Chem.* **1991**, *30*, 130. Behling, T.; Capparelli, M. V.; Skapski, A. C.; Wilkinson, G. *Polyhedron* **1982**, *1*, 840.

(32) Maatta, E. A.; Wentworth, R. A. D. *Inorg. Chem.* **1980**, *19*, 2597.

(33) Brynildson, M. E.; Bakac, A.; Espenson, J. H. *J. Amer. Chem. Soc.* **1987**, *109*, 4579. A bis($\mu$-peroxo) intermediate was suggested. $Cr(O_2)^{2+}$(aq) is, however, not strictly analogous because it is thought to be an $\eta^1$-superoxo complex of Cr(III) and not an $\eta^2$-peroxo complex of Cr(IV).

(34) (a) Lemenovskii, D. A.; Baukova, T. V.; Fedin, V. P. *J. Organomet. Chem.* **1977**, *132*, C14. (b) Lever, A. B. P.; Wilshire, J. P.; Quan, S. K. *Inorg. Chem.* **1981**, *20*, 761. (c) Balch, A. L.; Chan, Y.-W.; Cheng, R.-J.; La Mar, G. N.; Latos-Grazynski, L.; Renner, M. W. *J. Am. Chem. Soc.* **1984**, *106*, 7779. (d) Devore, D. D.; Maatta, E. A. *Inorg. Chem.* **1985**, *24*, 2846. (e) LaPointe, R. E.; Wolczanski, P. T.; Mitchell, J. F. *J. Am. Chem. Soc.* **1986**, *108*, 6382. (f) Groves, J. T.; Ahn, K.-H. *Inorg. Chem.* **1987**, *26*, 3831. (g) Morse, D. B.; Rauchfuss, T. B.; Wilson, S. R. *J. Am. Chem. Soc.* **1988**, *110*, 8234. (h) Egan, J. W., Jr.; Haggerty, B. S.; Rheingold, A. L.; Sendlinger, S. C.; Theopold, K. H. *J. Am. Chem. Soc.* **1990**, *112*, 2445.

(35) Ledon, H.; Bonnet, M.; Lallemand, J.-Y. *J. Chem. Soc., Chem. Commun.* **1979**, 702.

(36) The reaction has been proposed to involve a Mo(IV) peroxo complex as an intermediate (Ledon, H. J.; Bonnet, M.; Galland, D. *J. Am. Chem. Soc.* **1981**, *103*, 6209), which would make it analogous to the cases discussed above. However, no evidence for this intermediate was presented, and the fact that the reaction was photochemical and involves concomitant loss of $O_2$ complicates comparisons to the systems discussed here. It is also not clear that the symmetry arguments presented will apply given the unusual nonoctahedral stereochemistry of the porphyrin complexes.

(37) Chisholm, M. H.; Folting, K.; Huffman, J. C.; Kirkpatrick, C. C. *Inorg. Chem.* **1984**, *23*, 1021.

(38) Presumably, the dithiocarbamate or pyrazolylborate complexes could draw on their $\sigma$-bonding electrons in an analogous, symmetry-allowed, fashion. However, such a transformation would form a Mo(IV) cis oxo imido or Re(V) *fac*-trioxo complex, where the filled d orbital would interfere with $\pi$ bonding and thus lower the favorability of the reaction.

the scope of these reactions. The intermediate $(HBpz_3)$-Re(O) does react with dioxygen, yielding the rhenium(VII) trioxo complex $(HBpz_3)ReO_3$. While this appears at first glance to be a simple mononuclear cleavage of dioxygen involving a four-electron oxidation of the rhenium center, the mechanism is in fact more complex. Both labeling studies and analysis of the gases produced in the reaction show that only one of the two oxygen atoms added to the rhenium comes from molecular oxygen, with the second atom resulting from reduction of an oxalate ligand. The failure of $(HBpz_3)Re(O)$ to cleave dioxygen without assistance, despite a large thermodynamic driving force, may indicate a general symmetry-derived restriction on this reaction, which could explain why the four-electron reduction of $O_2$ at a single site remains elusive.

**Acknowledgment.** We thank Dr. Rasmy Talaat for obtaining the FAB mass spectra and Dr. Sue C. Critchlow for assistance with the X-ray crystallography. This work was supported by the National Science Foundation and by the donors of the Petroleum Research Fund, administered by the American Chemical Society.

**Supplementary Material Available:** Tables of data collection and refinement details, atom positional and isotropic thermal parameters, anisotropic thermal parameters, hydrogen atom parameters, bond distances and angles, and torsional angles (7 pages). Ordering information is given on any current masthead page.